Fluxes of CO_2 between the atmosphere and the ocean during the POMME project in the northeast Atlantic Ocean during 2001

Melchor González Dávila and J. Magdalena Santana-Casiano

Facultad de Ciencias del Mar, Universidad de Las Palmas de Gran Canaria, Las Palmas, Spain

Liliane Merlivat

Laboratoire d'Océanographie Dynamique et de Climatologie/Centre National de la Recherche Scientifique, Université Paris VI, Paris, France

Leticia Barbero-Muñoz and Evgeny V. Dafner

Facultad de Ciencias del Mar, Universidad de Las Palmas de Gran Canaria, Las Palmas, Spain

[1] In the eastern North Atlantic, carbon dioxide fugacity (fCO$_2$) in the upper mixed layer and discrete pH and total alkalinity measurements in the upper 2000 m were studied during three cruises (winter, spring, and summer 2001) within the framework of the Programme Océan Multidisciplinaire Méso Echelle (POMME) project. This extensive region is located between 39° and 45°N and 16° and 21°W. The mesoscale variability of fCO$_2$ on the sea surface and in the atmosphere during each season was determined to understand the mechanisms of evolution that control the spatial and temporal variability of fCO$_2$ together with an estimation of the fluxes of CO_2 between the atmosphere and the ocean. If we consider the observation to be 22 days per cruise, the region was in-taking 0.30 Tg C during the winter cruise and 0.36 Tg C during the spring cruise, whereas it was out-gassing 0.07 Tg C during the summer cruise. These values are clear indications that the area is acting as a sink of CO_2 on an annual scale, with an estimated flux value of -1.1 mol m^{-2} yr^{-1}, which is over twice as much as the mean global flux of -0.5 mol m^{-2} yr^{-1} (Takahashi et al., 2002). The changes with time observed in the fCO$_2$ values over the surface layer between the winter and the spring cruises have been described considering thermodynamics, gas exchange, water transport, and biological activity in the area. The estimation of the subduction of inorganic carbon yielded a value of 0.25 Pg C yr^{-1}, which is approximately 10% of the global net oceanic CO_2 sink flux.

Citation: González Dávila, M., J. M. Santana-Casiano, L. Merlivat, L. Barbero-Muñoz, and E. V. Dafner (2005), Fluxes of CO_2 between the atmosphere and the ocean during the POMME project in the northeast Atlantic Ocean during 2001, *J. Geophys. Res.*, *110*, C07S11, doi:10.1029/2004JC002763.

1. Introduction

[2] The French research project Programme Océan Multidisciplinaire Méso Echelle (POMME) was developed to understand the subduction mechanisms of the $11°-12°$C mode water in the northeast Atlantic. One of the most important objectives of this program was to understand how subduction of this water mass affects biological processes and the carbon budget in the northeast Atlantic whilst describing the fate of organic matter after the subduction. The carbon dioxide system in the area was studied in order to evaluate the behavior of the ocean in relation to the carbon dioxide exchange between the atmosphere and the ocean itself.

[3] The North Atlantic Ocean is known to be an important sink area for carbon dioxide [*Takahashi et al.*, 1995, 2002]. This conclusion was reached as the result of studies, which consider data from different cruises over the whole of the Atlantic Ocean [see *Takahashi et al.*, 1997, 1999, 2002]. These authors indicated the presence of strong sink areas in the transition zone between the subtropical gyres and subpolar waters, i.e., between $40°-60°$N and $40°-60°$S. According to *Takahashi et al.* [2002], the CO_2 uptake in the gyres ($14°-50°$N and $14°-50°$S) represents 56% of the total ocean uptake. However, there is no mesoscale study for the eastern part of the Atlantic Ocean with sufficient resolution to provide data with respect to the seasonal variability of the area. This transition zone is characterized by a thick mixed layer in the late winter in the north and relatively shallow mixed layers in the south [*van Aken*, 2001; *Mémery et al.*, 2005]. The cooling effect on the warm waters together with the biological drawdown of CO_2 in the

nutrient-rich subpolar water may account for the low fCO$_2$ (fugacity of carbon dioxide) values present in these surface waters. The seasonal and geographical variations in the surface water fCO$_2$ are easily superior to those observed for the atmospheric fCO$_2$, and therefore, the magnitude and direction of the air-sea CO$_2$ transfer flux is mainly governed by the oceanic fCO$_2$. In the mixed layer, the fCO$_2$ is affected by seasonal changes in temperature, total CO$_2$ concentration and alkalinity. There are several elements which regulate the seasonal variability of CO$_2$ in surface sea waters: physical processes, including the mixed layer thickness, biologically mediated processes and chemical processes affected by the upwellings of subsurface water, which are enriched in dissolved inorganic carbon and nutrients. In this paper, we present results of the sea surface fCO$_2$ in the transition zone between 16°W and 21°W in the North Atlantic over three seasons, distinguishing the seasonal biological effects from those due to seasonal temperature changes.

2. Experimental Procedure

2.1. Field Study

[4] The seasonal variability of the carbonate system properties was studied in an extensive region of the northeast Atlantic Ocean (∼550 by 750 km) between 39°N and 45°N and 16°W and 21°W, within the framework of the French oceanographic program POMME (Figure 1). Various phytoplankton conditions were studied over three seasons in the year 2001: prebloom (the winter cruise, 2–26 February), bloom (the spring cruise, 26 March to 13 April), and the postbloom conditions (the summer cruise, 22 August to 12 September).

[5] The inorganic carbon system variables, together with the physical and other biogeochemical characteristics, were ascertained over the three first legs of each cruise (http://www.lodyc.jussieu.fr/POMME). For the carbonate system variables, continuous underway fCO$_2$ determinations in the surface seawater and in the atmosphere were performed with minute and hourly resolutions, respectively. At the same time, the surface salinity and temperature (SST) were measured with a thermosalinograph SBE 21, and meteorological data was acquired through the shipboard station [*Caniaux et al.*, 2005]. Besides, discrete samples were collected down to a depth of 2000 m with a Seabird SBE 9 CTD sampler equipped with 24 12 L Niskin bottles for pH and total alkalinity (A_T) analyses. Stations were located at 54 km intervals along latitude and longitude.

2.2. fCO$_2$ (Fugacity of Carbon Dioxide)

[6] The fCO$_2$ in the air and in the seawater surface was determined using a flow system similar to that designed by *Wanninkhof and Thoning* [1993] and developed by Frank J. Millero's group at the University of Miami. The equilibrator used was based on the design by R.F. Weiss and described by *Butler et al.* [1988] working at ambient pressure. The concentration of CO$_2$ in the air and in the equilibrated air sample was measured with a differential, nondispersive, infrared gas analyzer supplied by LI-COR™ (LI-6262 CO$_2$/H$_2$O Analyzer). The samples were analyzed wet and the signal was then corrected for water vapor using the water channel of the LI-COR detector. The instrument was operated in the absolute mode and gathered CO$_2$ concentrations

directly from the detector. Atmospheric air was pumped at the bow of the ship and measured every hour. The nonlinear detector response was checked by measuring two different standard gases with mixing ratios of 348.55 and 520.83 ppmv (μmol/mol) CO$_2$ in the air. These gases are traceable to the World Meteorology Organization (WMO) scale. The zero of the gas analyzer was set by means of synthetic air without CO$_2$ or H$_2$O. The water channel was adjusted by controlling the dewpoint value in the ambient conditions. Our system operates at a precision of under 1 μatm and is thought to be accurate, relative to the standard gases, to 2 μatm. The fugacity of CO$_2$ in the seawater and in the atmosphere was calculated from the measured xCO$_2$ (mol fraction of gas CO$_2$ corrected to dry air, at the atmospheric pressure and at the temperature of the seawater for the ocean value) following *Wanninkhof and Thoning* [1993].

2.3. pH$_T$

[7] The pH in the total scale, pH$_T$ (hereafter in mol kg^{-1} seawater), was measured following the spectrophotometric technique of *Clayton and Byrne* [1993] with the m-cresol purple indicator [*Dickson and Goyet*, 1994]. The value pH$_T$ − 25°C was used afterward to compute total dissolved inorganic carbon (C_T, see below). A system based on the one described by *Bellerby et al.* [1995] has been developed in our lab. The pH$_T$ measurements were carried out using a Hewllet Packard Diode Array spectrophotometer in a 25°C thermostatted 1 cm flow cell, with a Peltier system. Using a stopped flow protocol, seawater, previously thermostatted to 25°C, was analyzed for a blank determination at 730 nm, 578 nm and 434 nm. The flow was restarted and the indicator injection valve switched on to inject 10 μl of dye through a mixing coil (2 m). Three photometric measurements were carried out for each injection at different times after mixing in order to remove any dye effect from the seawater pH measurement.

[8] The method has a reproducibility of ±0.002 pH$_T$ units and the pH$_T$ measurements were shown to be internally consistent with other carbon dioxide measurements. We used the certified reference materials (CRM) provided by A. Dickson (SIO, La Jolla, CA, U.S.A) with known values of C_T and A_T, and calculated with the carbonic acid dissociation constants of *Mehrbach et al.* [1973] after *Dickson and Millero* [1987].

2.4. Total Alkalinity, A_T

[9] The alkalinity of seawater was determined through the titration of discrete seawater samples with two identical potentiometric systems as described in detail by *Mintrop et al.* [2000]. The performance of the titration systems was monitored through the titration of CRM (batches 49 and 50) that have known C_T and constant A_T values. The onboard precision of A_T analyses relative to CRM was ±1.4 μmol kg^{-1}.

[10] The total dissolved inorganic carbon was computed from A_T-pH$_T$ pairs for the water column samples and from A_T-fCO$_2$ pairs for the surface measurements. In both determinations, the carbonic acid dissociation constants of *Mehrbach et al.* [1973] after *Dickson and Millero* [1987] were used. Assuming that there exists a linear relationship between the alkalinity of discrete surface seawater (<10 m)
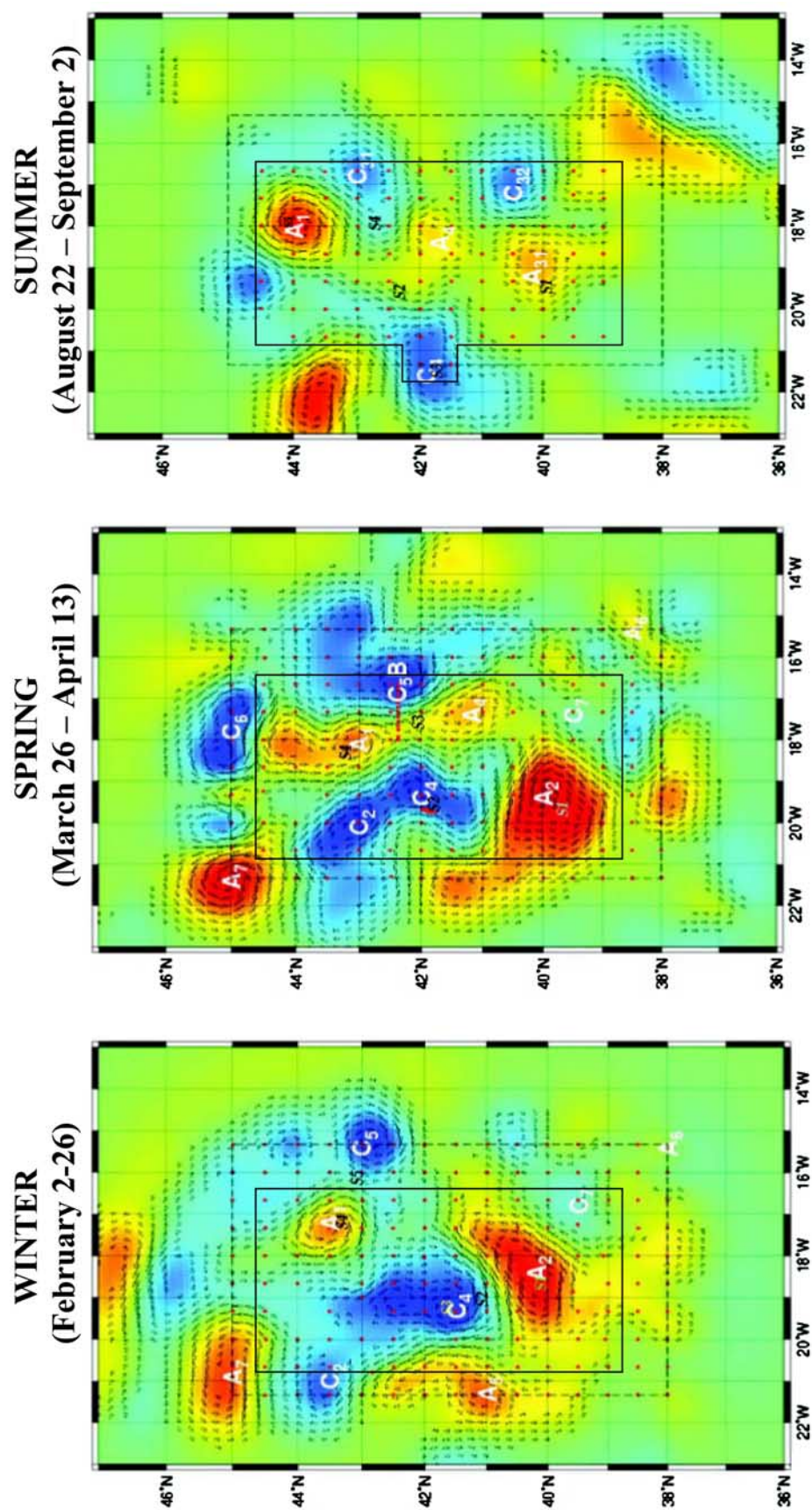
Figure 1

and the salinity over the three cruises, we obtained the following expression:

$$A_T = 107.5 + 62.59 * S \, (r^2 = 0.92, n = 212), \qquad (1)$$

with a standard error ±2.25 μmol kg^{-1}. Surface A_T was computed from salinity obtained from the continuous thermosalinometer system located at the seawater intake. Afterward, we used these high-resolution A_T and fCO$_2$ data for C_T calculation at the surface; the uncertainty of this C_T calculation was ±3.4 μmol kg^{-1}.

2.5. CO$_2$ Fluxes

[11] Finally, the CO$_2$ fluxes between atmosphere and ocean (mmol m^{-2} d^{-1}) were calculated using experimentally determined fCO$_2$ values in the atmosphere and in the ocean. The flux of CO$_2$ across the sea-air interface is the product of the gas transfer velocity, k (cm h^{-1}), the solubility of CO$_2$, s (mol kg^{-1} atm^{-1}), and the fCO$_2$ difference between the ocean and the atmosphere (fCO$_2$sw − fCO$_{2a}$, both in μatm):

$$F = 0.24 k \, \cdot \, s \, \cdot \, (f\text{CO}_2\text{sw} - f\text{CO}_{2a}). \qquad (2)$$

The transfer velocity relationship of *Wanninkhof* [1992] was used to provide CO$_2$ flux calculations:

$$k = 0.31 w_{10}^2 (Sc/660)^{-0.5}, \qquad (3)$$

where Sc is the Schmidt number for CO$_2$ calculated from its relation with temperature according to the polynomic fit given by *Wanninkhof* [1992] and w_{10} is the wind speed at a 10 m height (in m s^{-1}). Wind speed data were gathered at 1 min intervals from the meteorological station onboard in order to compute discrete fluxes. The atmospheric pressure values were obtained from our system. ECMWF sea surface stress (forecast) values extracted by Thierry Ludget (Meteo-France, Mercator project) and kindly provided by Dr. Assenbaum (LEGOS, Toulouse) were used to compute the transfer velocity coefficient (3) when overall fluxes were computed. The differences between wind values obtained at stations with duration longer than 6 hours and average ECMWF wind data integrated over 6 hours, were within ±2 m s^{-1}.

[12] In order to compute fluxes in the 5.5° × 4.0° POMME area, we used an ocean area of 2.03 10^{11} m^2.

3. Results and Discussion

3.1. fCO$_2$ in Relation to the Hydrological Features

3.1.1. Winter Conditions

[13] A complete description of the mesoscale features studied during the POMME experiment and the evolution of the same from one cruise to the next over the three cruises can be found elsewhere [*Reverdin et al.*, 2005; *Assembaum and Reverdin*, 2005; *Fernández et al.*, 2005a]. Briefly, the

POMME area is a transition zone between a rather deep, late winter mixed layer in the north and relatively shallow, mixed layers in the south. Figure 2 shows the mixed layer depth (MLD), the sea surface temperature, the salinity, the inorganic carbon normalized to a constant salinity of 35 (NC_T) and averaged over the mixed layer, and the surface fugacity of CO$_2$ distributions for the winter cruise. The averaged MLD during winter was 135 m, with an average value of 120 m to the south of 42°N and increasing up to 150 m to the north of 42°N (with values as high as 240 m in the northern part of the region).

[14] Saltier and warmer surface waters were observed to the south of about 41°N induced a strong decreasing gradient of potential density (σ$_θ$) southward. The σ$_θ$ changed from 26.9 kg m^{-3} at 42° to 26.8 kg m^{-3} at 40.5° N. Alternating cyclonic and anticyclonic gyres (Figure 1) featured a clearly identifiable signature on the MLD and SST distributions (Figure 2). The strong cyclonic eddy (C$_4$) approximately centered at 42°N and 19°W uplifts cold and nutrient rich water from a depth of about 100 m to the surface. Owing to this water displacement, a strong southward gradient was observed at 41°N between waters with low temperature and salinity and high NC_T, and waters with higher values of temperature and salinity and lower values of NC_T. The average C_T over the mixed layer (data not shown) was relatively constant throughout the area (2104 ± 4 μmol kg^{-1}), with the lowest values south of 41° (2101 ± 4 μmol kg^{-1}). After normalization, the average NC_T value above the mixed layer reached 2065 μmol kg^{-1} to the north of 41°, while to the south of 41°, the NC_T values were always under 2050 μmol kg^{-1}. Ten units of variability were observed close to 41°N, relating to the front zone (Figure 2). The presence of a deep thick mixed layer during winter conditions in the northern part favors the mixing with deeper Northeast Central Atlantic Water, enriched in total inorganic carbon.

[15] The presence of cyclonic eddies should also have affected the fCO$_2$ distribution. However, fCO$_2$ in these colder waters was not only affected by the temperature change that would reduce its value. These uplifted waters also have a higher total dissolved inorganic carbon content which may compensate said effect due to the temperature change. Moreover, new production and air-sea exchange would also affect the final surface distribution. Owing to these different inputs and to the resolution presented in the property distributions (Figure 2), not all of the features visible in the temperature fields are to be clearly observed in the surface distributions of the carbonate system variables. The sea surface fCO$_2$ throughout this cruise was 343 ± 6 μatm on average for the whole area, with a pronounced north-south trend: 350 μatm at 43°N, 340 μatm at 41°N, and 330 μatm south of 41°N (Figure 5). *Ríos et al.* [2005] found for the Azores area south of 40°N, an average value of 320 μatm in February 1998, which is in line with our observations. After normalization to a constant temperature of 14°C (the average SST value during the winter cruise),

---

Figure 1. Location of the Programme Océan Multidisciplinaire Méso Echelle (POMME) area (solid line) and conductivity-temperature-depth (CTD) casts station grid (dots inside the rectangle) over an output from the Soprane Circulation Model updated with CTD data from each cruise (M. Assenbaum, LEGOS/CNRS, Toulouse). The position of mesoscale eddies during each cruise is shown as C for cyclonic and as A for anticyclonic gyres.
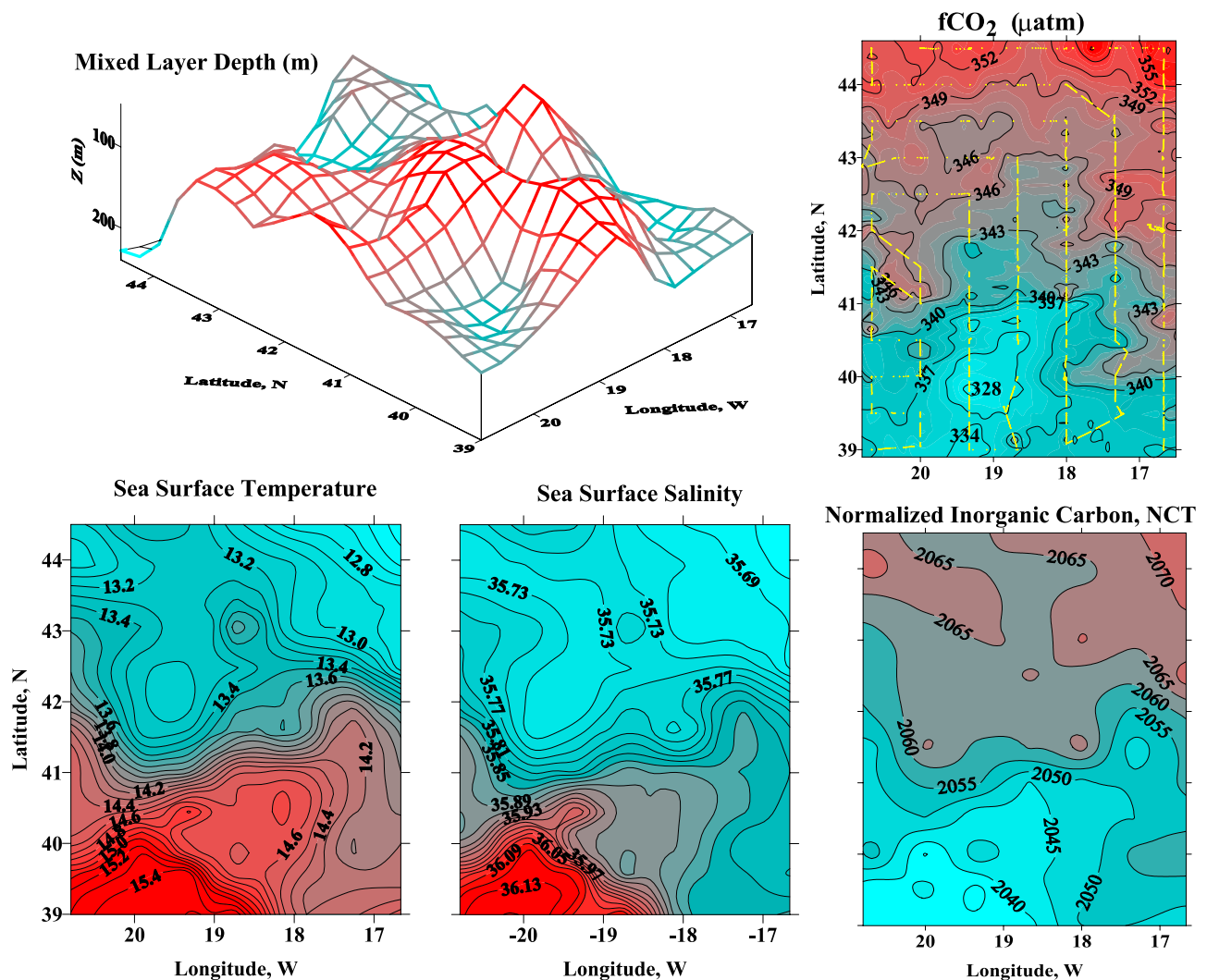
Figure 2. Characteristics of the sea surface properties obtained during the winter cruise: the depth of the mixed layer (m), sea surface temperature (°C), salinity, fugacity of carbon dioxide (μatm), and C_T normalized to a constant salinity of 35 (NC_T in μmol kg^{-1}) averaged over the depth of the mixed layer. Red and blue colors are used for the highest and lowest values of each panel, respectively.

following *Wanninkhof and Thoning* [1993], NfCO$_2$ ranged from 365 μatm at 42°N to 325 μatm south to 40.5°N (data not shown). Winter atmospheric fCO$_2$ stood at an average value of 370 ± 5 μatm (xCO$_2$ = 375 ± 2 ppmv) over the whole area during February 2001. This value is the same as the average value obtained in the Global View−CO$_2$ station at Terceira Island, Azores (xCO$_2$ = 374.2 ± 0.2 ppmv) for the same period (http://islscp2.sesda.com/ISLSCP2_1/html_pages/groups/carbon.html).

3.1.2. Spring Conditions

[16] During this period, the distribution of sea surface variables was approximately similar to that of the winter season (Figure 3). However, the mixed layer depth decreased from 130 m (the winter cruise) to around 50 m (the spring cruise), with values in the north being over twice the values computed for the south (65 m vs. 31 m). North of 41°N three cyclonic eddies were observed, two centered around 43°N (C$_2$) and 42°N (C$_4$) and 20°W, and the other centered around 43°N and 17°W (C$_5$B). In all of them, the temperature, as averaged over the MLD, decreased to

13.1°C. An anticyclonic eddy was found between cyclonic eddies C$_2$ and C$_5$ (43°N and 18°N) with significantly higher averaged temperature over the MLD (>14°C). South of 41°N the temperature increased from 14.3°C to 15.5°C, and the presence of a strong anticyclonic eddy centered at 40°N, 20°W (A$_2$) was to be observed.

[17] To the north of 42°N, mixed layer−averaged NC_T value was 2058 and 2050 μmol kg^{-1} in the cyclonic and anticyclonic eddies respectively, with a mean value of 2053 μmol kg^{-1} (Figure 3). NC_T values in the south were 2041 μmol kg^{-1} on average, with minimum values around 2025 μmol kg^{-1} in the anticyclonic eddy A$_2$. However, we should remember that the spring cruise took place between the end of March and 12 April, and that the southwest region was studied at the end of the cruise (10−12 April). During the whole period of the cruise, rapid increases in fluorescence were to be observed in various regions of the POMME area, due to the beginning of the spring bloom [*Merlivat et al.*, 2001]. Therefore the spring cruise did not offer similar bloom conditions over the whole domain.
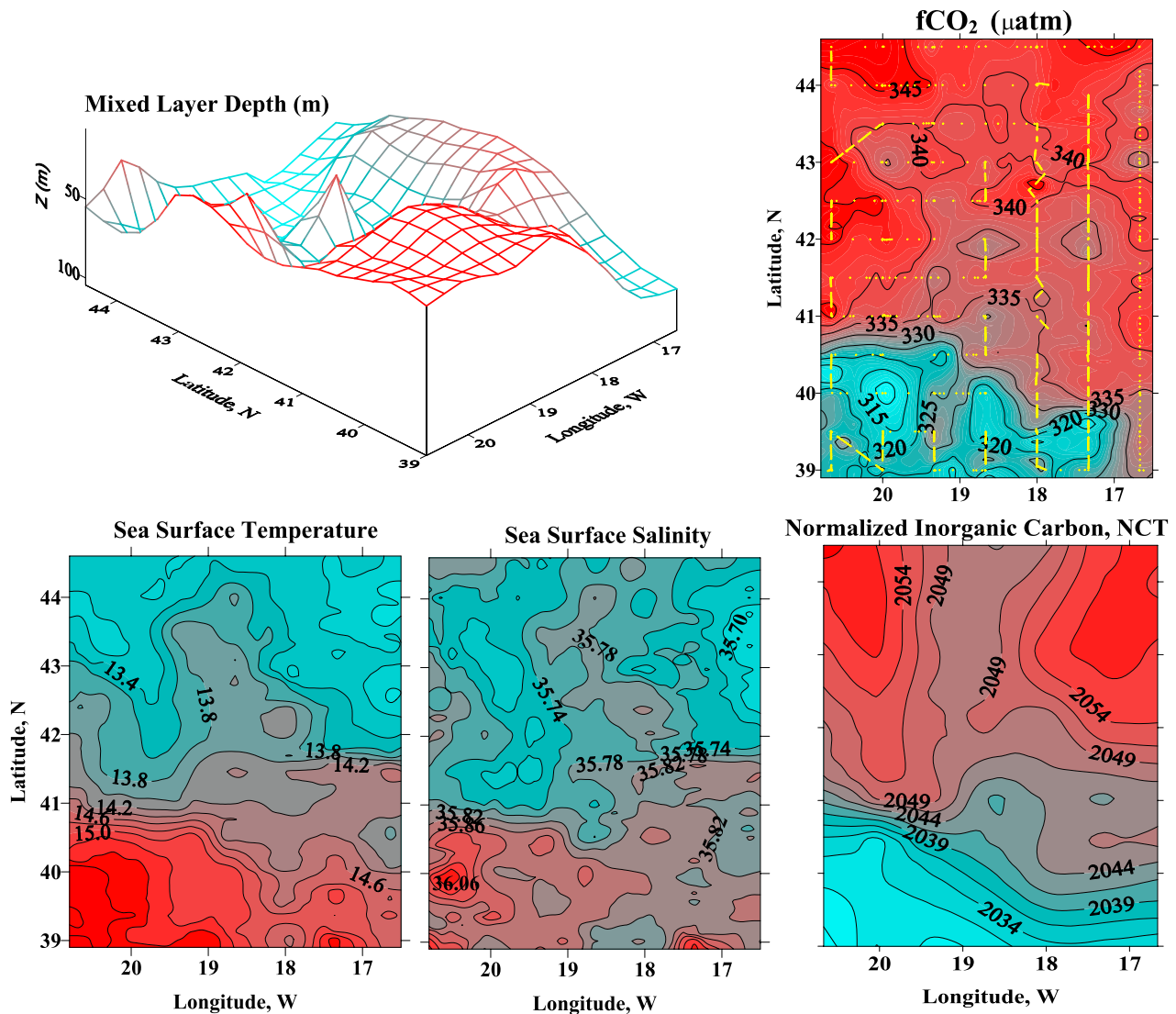
Figure 3. Same as Figure 2, except for the spring cruise.

[18] Likewise, the fCO$_2$ showed a north-south trend with values decreasing from 342 to 310 µatm (Figure 3). As was already indicated in the case of the winter cruise, the presence of cyclonic eddies in the spring cruise was not clearly reflected in the fCO$_2$ distribution (for example at 43°N and 42°N by 20°W), which is related to low net effects on the final value. Moreover, the lowest values (around 300 µatm) were to be found in the southwest corner of the POMME area, and were related to bloom conditions. This trend did not disappear after normalization to a constant temperature of 14°C (to account for any thermodynamic effects on the CO$_2$ variability), and indeed, the NfCO$_2$ distribution in this area reached the lowest value (<286 µatm), indicating a significant drawdown of CO$_2$ by biologically mediated activity (biological pump). The spring atmospheric fCO$_2$ concentration was 372 ± 2 µatm (xCO$_2$ = 376 ± 1 ppmv) on average over the whole area, being similar to fCO$_2$ values obtained at the Azores atmospheric station (xCO$_2$ = 375.9 ± 0.3 ppmv, see above).

3.1.3. Summer Conditions

[19] During the summer cruise the mixed layer depth was reduced to 20 m (Figure 4) and, to the east of 18°W,

it surfaced due to the presence of two cyclonic eddies, centered at 40°N, 17°W (C$_{32}$) and 43°N, 17°W (C$_{31}$) (Figure 1). The sea surface temperature showed a large variation of 1°C at 43°N, particularly noticeable on account of the compressed isotherms in a frontal zone located approximately along 43°N. The north-south transition zone had moved northward, from around 41°–42°N during late winter and spring to 43°N during the summertime. The temperature at 20°W changed from 19.8°C at 44°N to 23.2°C at 39°N. The increase in temperature between spring (March–April) and late summer (September) was close to 8°C to the south of 42°–43°N, and about 6°C to the north of 43°. This range describes the seasonal temperature variability for the area, in spite of the high variability associated to the mesoscale activities in the POMME area.

[20] As was expected [*González Dávila et al.*, 2003], total inorganic carbon in the mixed layer decreased from 2104 µmol kg^{-1} (winter cruise) to 2059 µmol kg^{-1} (summer cruise) on average, mainly due to the variability of physicochemical properties (T and S generally referred to as "the thermodynamic effect"), and biological activ-
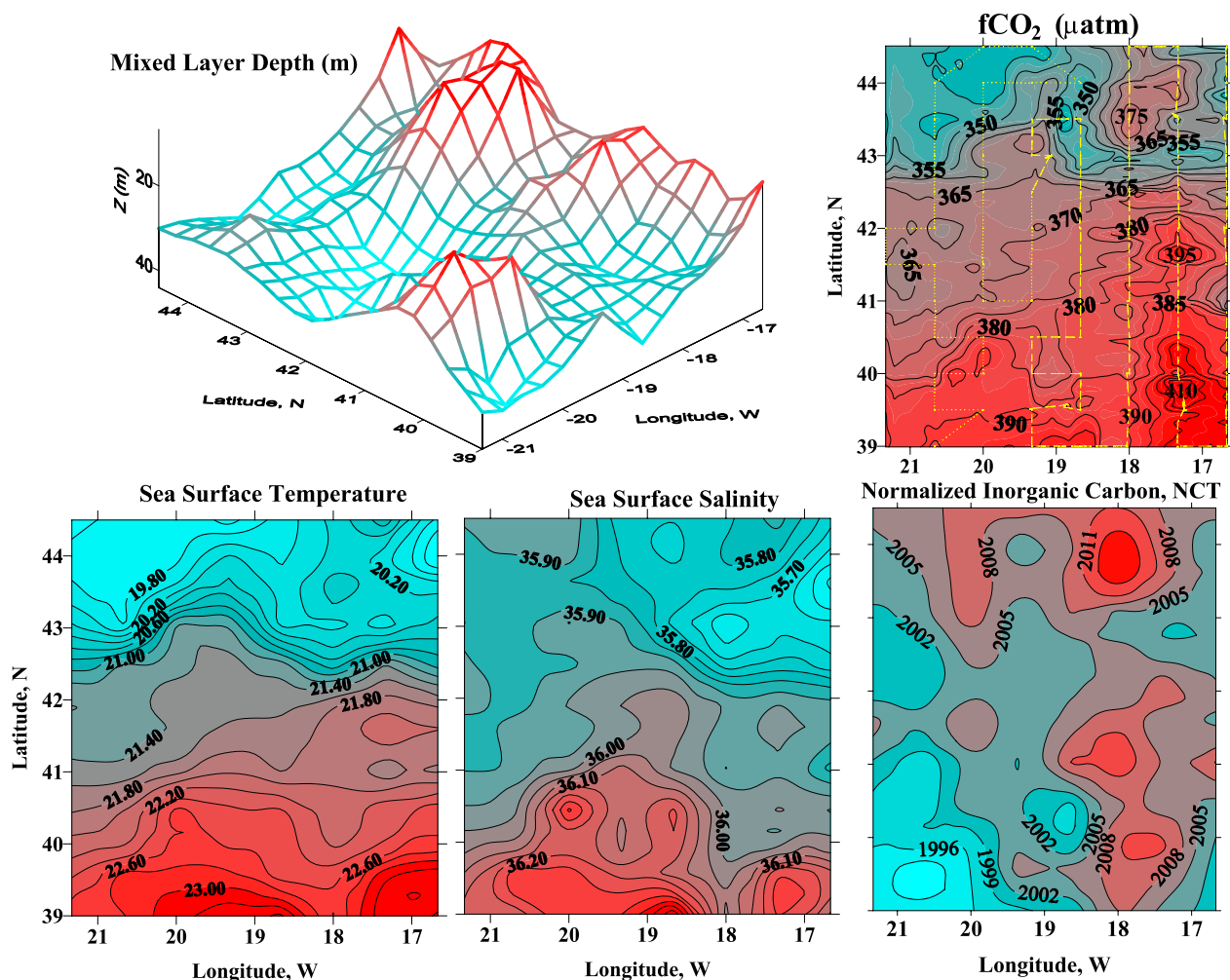
Figure 4. Same as Figure 2, except for the summer cruise.

ity. After normalization, the NC_T reached a value of 2005 μmol kg^{-1} during the summer cruise, which was 50 units lower than in the winter cruise (Figure 4). A similar seasonal variability (45 μmol kg^{-1} yr^{-1}) was observed for the Azores area using data from several cruises carried out in different years [*Ríos et al.*, 2005] and at the BATS station time series [*Bates*, 2001]. The averaged values for each season were affected by the mesoscale activity. The presence of a strong cyclonic eddy during the summer in the northeast area, at around 43°N, 17°W, with low temperature and salinity over the first 100 m, made both the NC_T and the fCO$_2$ higher than those observed to the west of 18°W. South of 43°N, the surface fCO$_2$ values increased, reaching 400 μatm south of 40°N. A similar value was presented by *Ríos et al.* [2005] for the data collected south of 40°N in September 1998. The presence of the cyclonic eddy near 40°N, 17°W, also contributed to the observed high fCO$_2$ and averaged NC_T values. North of 42°N, the fCO$_2$ values increased in 19 μatm relative to the value observed during the spring cruise. The atmospheric fCO$_2$ during September 2001 was 358 ± 4 μatm (xCO$_2$ = 366 ± 2 ppmv) in this study, and 365.7 ± 0.5 ppmv at the Azores atmospheric station (see above), 12 μatm lower than the values observed during the winter and spring cruises.

3.2. Spatial and Seasonal Heterogeneities of fCO$_2$

[21] In order to establish the spatial heterogeneities of the fCO$_2$ between the three seasons, the fCO$_2$ in seawater was averaged every 0.5° in latitude and the values were plotted in Figure 5, together with the average atmospheric fCO$_2$ values. As was previously described, surface seawater fCO$_2$ was always higher in the winter than in the spring cruise (5–10 μatm, on average), but both were lower than in the summer cruise (30–90 μatm, on average). The lowest values during the winter and spring cruises were always observed south of 41°–42°N, where, for example, at 39.5°N, differences with respect to values at 42°N could reach up to 20–25 μatm. Between the spring and summer cruises, the differences increased from 25 to 60 μatm. From February to April atmospheric values were always higher than seawater values, with the highest gradients observed toward the south.

[22] During the summer cruise, the atmospheric fCO$_2$ values were higher than seawater values only to the north of 43°N, indicating that this area was acting as a sink of atmospheric CO$_2$. The fCO$_2$ gradients between the atmosphere and the seawater were much more important to the south, reaching up to 35 μatm at 39.5°N, showing that in the latter area the ocean was acting as a source of CO$_2$ for the atmosphere. Equilibrium was never observed between
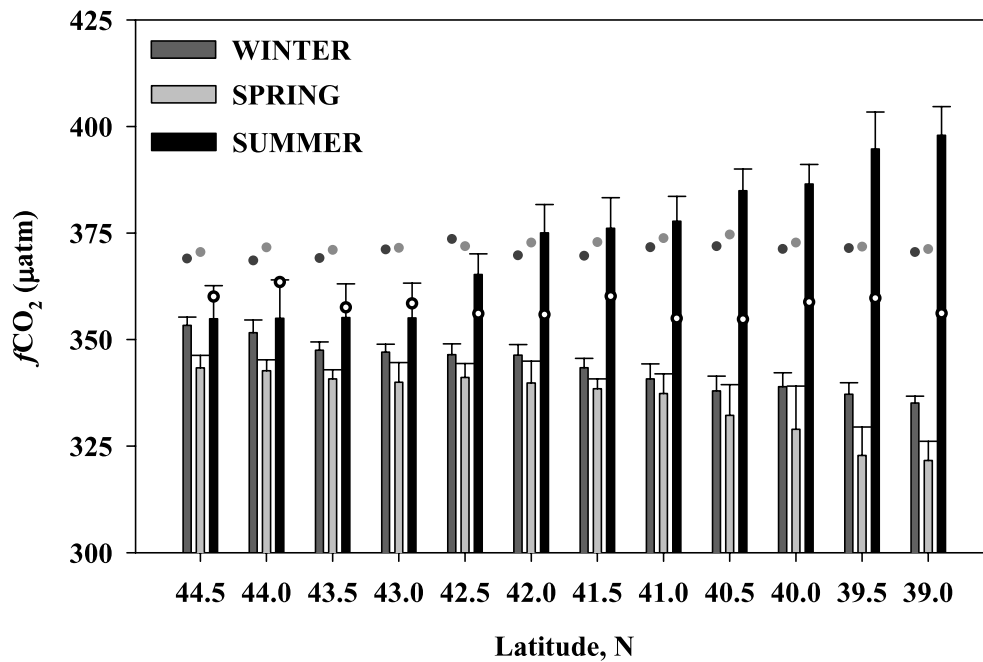
Figure 5. Bar diagram for averaged continuous underway fCO$_2$ measurements (µatm) for each season, determined for every 0.5° latitudinal zone. Dotted points are the averaged atmospheric fCO$_2$ values for each section and season.

the atmospheric and sea surface fCO$_2$ during the winter and spring cruises to the north of 42°N, where subduction of surface water was expected [*Paillet and Arhan*, 1996]. Only during the summer cruise, and related to the lower atmospheric fCO$_2$ content, equilibrium conditions were to be assumed, north of 43°N. In all other cases, the ΔfCO$_2$ was always higher than 15 µatm in the winter and higher than 25 µatm in the spring. In this area, low fCO$_2$ concentrations could be attributed to the juxtaposition of the cooling of warm waters and the biological drawdown of fCO$_2$ in the nutrient-rich subpolar waters. Moreover, high wind speeds over these areas with low fCO$_2$ concentrations could increase the rate of CO$_2$ uptake by the oceanic waters.

3.3. Estimation of the Net Sea-Air CO$_2$ Flux

[23] Net fluxes of CO$_2$, FCO$_2$, were calculated using the appropriate *Wanninkhof* [1992] relationship (see section 2.5) and by considering either the wind speed recorded on the oceanographic vessel, or the ECMWF analyzed wind at 10m (data provided by the Laboratoire d'Etudes en Gèophysique et Océanographie Spatiale, LEGOS, Toulouse). Owing to the variable wind conditions over the 20–25 days of each cruise, ECMWF wind data instead of shipboard wind data were considered in this study. The fCO$_2$ values determined for each position during each cruise were presumed to be representative of the value for the whole cruise. As it was indicated above, the values determined at the end of the spring cruise might not have been representative of the situation at the beginning of the cruise. Figure 6 shows the daily average value of FCO$_2$ for each cruise for the whole area using four wind measurements per day (6 hour intervals) with a 0.5° × 0.5° resolution. Figure 6 also depicts the average values, obtained north and south of 42°N. Our calculations suggest that during the

winter cruise, the ocean was in-gassing CO$_2$ at a rate of 5.55 mmol m^{-2} d^{-1} with the highest values determined between 5 and 8 February due to the strong winds in the area (over 15 m s^{-1}). After 12 February, the average flux halved (−2.91 mmol m^{-2} d^{-1}) corresponding with the decrease in wind speed. The observed differences between the areas located north and south of 42°N were ascribed to the low ΔfCO$_2$ values and bear less relation to the differences in wind speed.

[24] During the spring cruise, the highest gradient of fCO$_2$ observed in the southwest corner, slightly increased the computed fluxes. A great variability in the FCO$_2$ was observed over the 21 days of the cruise in line with the variability of the wind field. The CO$_2$ flux varied from −1 to −16 mmol m^{-2} d^{-1} with an average value of −6.73 mmol m^{-2} d^{-1} for the whole POMME area. These variations were related to wind strength. Strong differences in the wind field and the ΔfCO$_2$ to the north and south of 42°N explained the variability observed in the fluxes in both areas. Differences of up to 7 mmol m^{-2} d^{-1} were determined on the same day, to the north and to the south of 42°N.

[25] During the summer cruise, the area acted as a scant source of CO$_2$, out-gassing CO$_2$ at a rate of 1.4 mmol m^{-2} d^{-1} on average (Table 1). However, to the north of 42°N there was a nil (or slightly negative) FCO$_2$ due to the small negative ΔfCO$_2$ values. South of 42°N, the area acted as a source of CO$_2$ (2.9 ± 2.0 mmol m^{-2} d^{-1}) with values of up to 6 mmol m^{-2} d^{-1} favored by the strong wind conditions (Figure 6 and Table 1).

[26] Considering the 5.5° × 4° POMME area and the 22 days of observations for each cruise, we estimated that the area was in-taking 0.30 Tg C during the winter cruise, 0.36 Tg C during the spring cruise and out-gassing 0.07 Tg C during the summer cruise. These values clearly show that
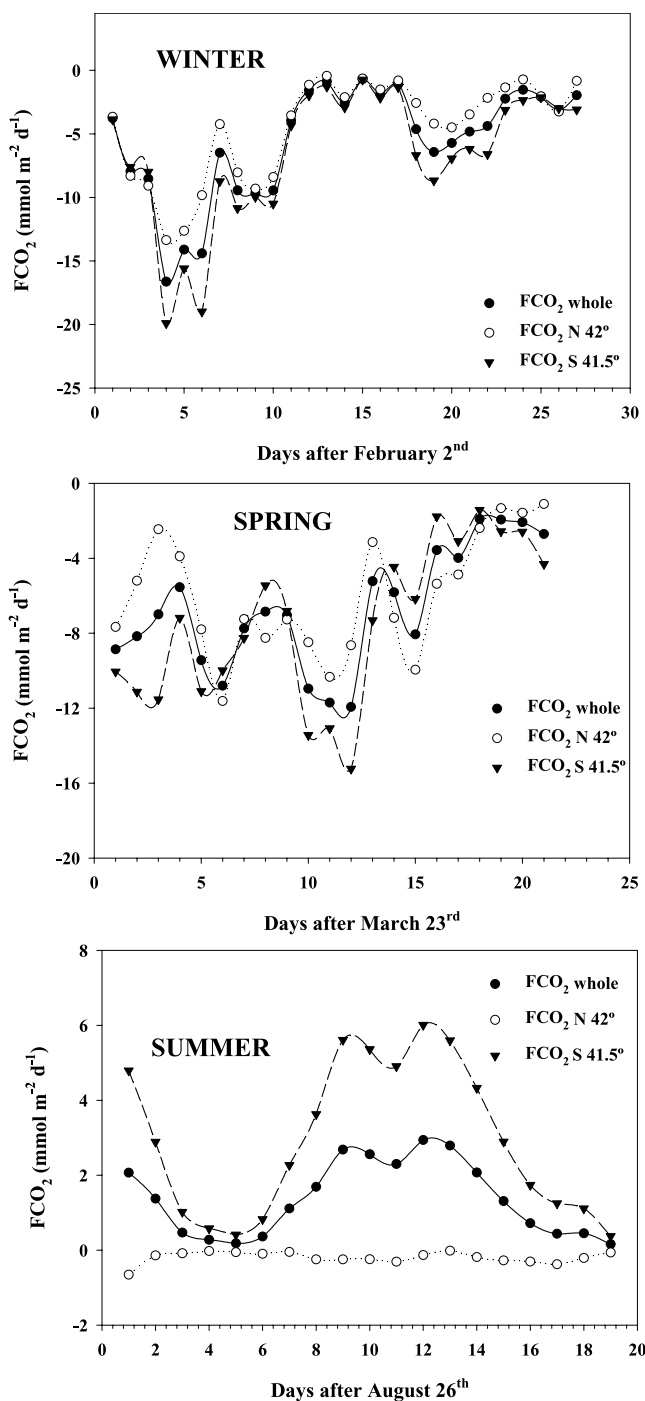
Figure 6. Temporal evolution of the flux of CO_2 for the three seasons calculated with the appropriate *Wanninkhof* [1992] relationship and considering climatological wind field data (four observations per day in a $0.5° \times 0.5°$ resolution). For the flux estimates the whole POMME area was divided into two parts: to the north and to the south of $42°N$.

the area was acting globally as a sink for atmospheric CO_2. From the end of April to the middle of May, when the second leg of the spring cruise was effected, chlorophyll concentration increased all over the POMME area, suggesting an increase in the ΔfCO_2 values between the ocean and

the atmosphere. Wind conditions were, to a large extent, similar to those found during the first leg. In such a situation, the FCO_2 value should have increased.

[27] In order to estimate an FCO_2 value from the winter (February) to the summer (September) cruises, a harmonic function between the points was considered (Figure 7), forcing a minimum value at the end of April in accordance with the Carioca buoy determinations [*Mémery et al.*, 2005]. Our fit was improved by considering data from previous cruises in this area (CARINA project, http://www.ifm.uni-kiel.de/fb/fb2/ch/research/carina). A similar yearly increase in the fCO_2 both in the atmosphere and in the ocean, was assumed for these data included in Figure 7. Considering this, our data and data from a cruise carried out in September 1996 (Cruise 74JC9609 Lefevre, Aiken, CARINA project) differed by 3.5 µatm. The transfer velocity coefficient was computed using ECMWF wind data and integrating the values for the time that the cruise spent in the POMME area (4 days on average). From these data, an averaged FCO_2 value of -0.88 mol m^{-2} was estimated between 1 February and 15 September, that gives an air-sea flux of zero at the end of July. This average value corresponds to an uptake of 2.13 Tg C over the POMME area and over 227 days (1 February–15 September). We assumed the summer value in the year 2000 to be similar to the one of summer 2001, used data from previous cruises, and forced a maximum value at the beginning of October (following sea surface temperature values [*González Dávila et al.*, 2003]). An averaged value of -1.1 mol m^{-2} yr^{-1} (or 2.71 Tg C) can be estimated, with an average daily intake of -3.0 mmol m^2 d^{-1}. If we again split the POMME area into two regions, north and south of $42°N$, the values we obtained were -1.3 and -1.0 mol m^{-2} yr^{-1}, respectively. According to *Takahashi et al.* [2002], a mean annual net air-sea flux of -1 mol CO2 m^{-2} yr^{-1} for 1995 was obtained for the area where the POMME project was conducted.

3.4. Temporal Changes in the fCO_2

[28] The changes with time of the fCO_2 observed in the surface layer between the seasons, $\Delta f/\Delta t$, were related to variations of fCO_2. The effect of sea surface temperature at constant chemistry ($\delta f/\delta T$) and the changes in the total CO_2 concentration in seawater as a result of sea-air CO_2 flux while other variables are kept constant ($\delta f/\delta F$), were considered. A residual term, ($\delta f/\delta R$), includes the combined effects of biological activity, horizontal and vertical transport and mixing (the last of these physical processes was not taken into account since the mixed layer depth, Z, decreased between cruises) at constant temperature and air-sea exchange [*Poisson et al.*, 1993] or

$$\Delta f/\Delta t = (\partial f/\partial T)(\Delta T/\Delta t) + (\partial f/\partial F)(\Delta F/\Delta t) + (\partial f/\partial R)(\Delta R/\Delta t). \tag{4}$$

Figures 2–4 demonstrate the high fCO_2 variability between different seasons and the spatial variability within each season. Following the same procedure used for the fCO_2 data treatment, in our study, we have considered the average values for the whole area and those for the regions to the north and south of $42°N$. The results in Table 1 summarize the averaged values over the mixed layer depth for each cruise, while Table 2 represents averaged, observed and

Table 1. Mean Values of Temperature (T), Salinity (S), Mixed Layer Depth (Z), fCO$_2$, C_T and Air-Sea Flux of CO$_2$ (FCO$_2$) for the Three Cruises for the POMME Area and for the Regions North of 42°N and South of 42°N

Season/Cruise	Area	T, °C	S	Z, m	fCO$_2$, μatm	C_T, μmol kg^{-1}	FCO$_2$, mmol m^{-2} d^{-1}
Winter	whole	13.86	35.806	135	343.1 ± 5.7	2086 ± 5	−5.55 ± 4.4
	north of 42°	13.18	35.709	151	347.9 ± 3.8	2089 ± 3	−4.5 ± 3.9
	south of 42°	14.32	35.873	120	339.8 ± 4.2	2084 ± 3	−6.6 ± 5.2
Spring	whole	14.06	35.781	47	334.2 ± 9.4	2090 ± 4	−6.7 ± 3.3
	north of 42°	13.44	35.727	65	340.9 ± 3.9	2096 ± 6	−6.0 ± 3.2
	south of 42°	14.48	35.819	31	329.4 ± 9.3	2085 ± 3	−7.5 ± 4.1
Summer	whole	21.87	35.940	28	374.7 ± 8.9	2053 ± 5	1.4 ± 1.0
	north of 42°	20.99	35.772	28	359.9 ± 8.1	2047 ±7	−0.24 ± 0.16
	south of 42°	22.43	36.048	28	388.4 ± 9.2	2057 ± 4	2.9 ± 2.0

determined changes for each parameter in between cruises. The temperature effect on the fCO$_2$ in isochemical conditions (∂ln fCO$_2/\partial$T) was calculated considering a 4.23% °C^{-1} increase with temperature over the initially averaged fCO$_2$ for each cruise [*Takahashi et al.*, 1993]. The daily change of the surface fCO$_2$ due to air-sea exchange was determined by *Bakker et al.* [1997]:

$$(\delta f / \delta F) = F_{av}\, \beta\, fCO_{2sw} TC_T^{-1}, \qquad (5)$$

with β the computed buffer or Revelle factor for each period, and TC_T (mol m^{-2}), the average amount of total dissolved inorganic carbon in the mixed layer per area unit. TC_T was estimated as the product of the average C_T in the mixed layer, the mixed layer thickness and the density, considering a linear evolution between cruises.

[29] Between February and April (49 days), the fCO$_2$ decreased slightly (8.9 ± 6.3 μatm), following a similar decreasing pattern over the whole area. The 0.2°C increase in temperature as well as the in-gassing of CO$_2$, increased the daily change of the fCO$_2$, so that it reached a residual value of −0.35 μatm d^{-1} (Table 3). This daily residual of fCO$_2$, ($\delta f/\delta R$), was converted into a net residual daily change of dissolved inorganic carbon over the depth of the mixed layer, RfCO$_2$:

$$R_{fCO_2} = (\delta f / \delta R) TC_T\, \beta^{-1}\, fCO_{2sw}^{-1}. \qquad (6)$$

RfCO$_2$ yields a value of −19.1 mmol m^{-2} d^{-1} (indicating a drawdown of 2.3 Tg C during the 49 days in the 2.03 ×
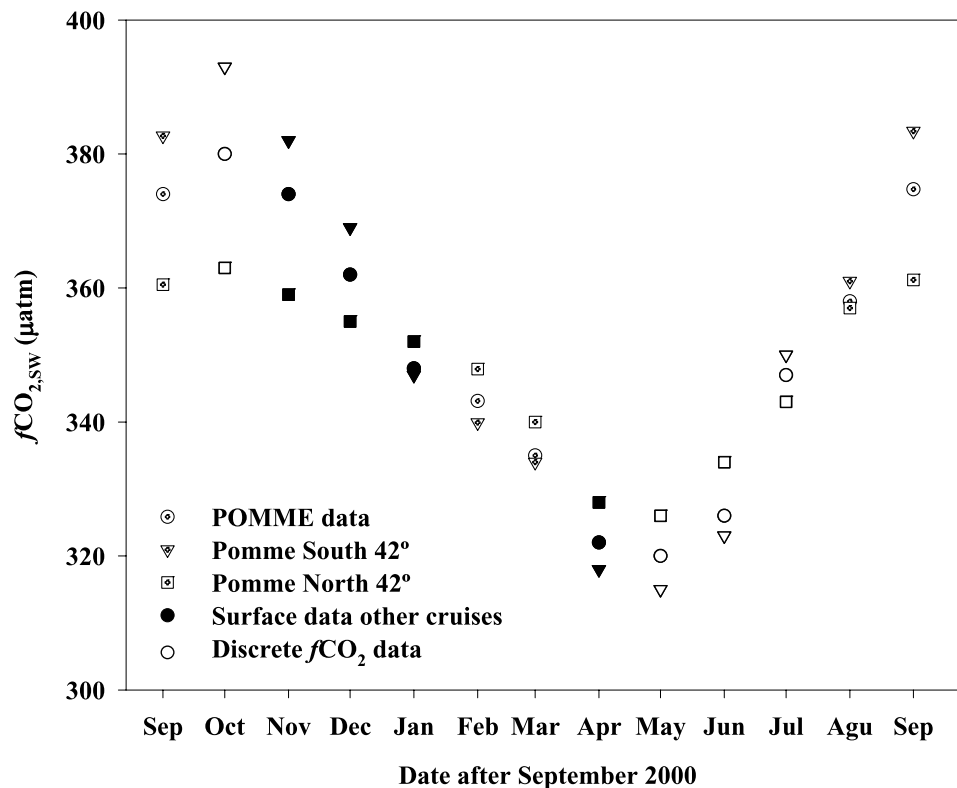

Figure 7. fCO$_2$ values used for the annual flux estimates in the POMME region. Open symbols with dots are underway fCO$_2$ data from POMME cruises, closed symbols correspond with data computed using fCO2 surface values, and open symbols correspond with data computed using discrete carbon system parameters, both of them from cruises carried out in the area in previous projects (http://www.ifm-kiel.de/fb/fb2/ch/research/carina).

Table 2. Changes of Surface Water Properties in Between Cruises for the POMME Area and for the Regions North of 42°N and South of 42°N[a]

Season/Cruise	Area	Δt, days	Z, m	ΔT, °C	fCO$_2$, µatm	ΔfCO$_2$, µatm	β	C_T, µmol kg^{-1}	ΔC_T, µmol kg^{-1}	FCO$_2$, mmol m^{-2} $^{-1}$	TC_T, mol m^{-2}
Winter/spring	whole	49	91	0.2 ± 0.3	338.6 ± 7.6	−8.9 ± 6.3	10.7	2088 ± 6	3.9 ± 6.2	−6.2 ± 4.1	196
	north 42°	49	108	0.24 ± 0.3	344.4 ± 3.8	−7.0 ± 3.8	11.0	2094 ± 4	7.0 ± 5.2	−5.2 ± 3.5	232
	south 42°	49	76	0.17 ± 0.4	334.6 ± 6.8	−10.4 ± 7	10.5	2084 ± 5	0.9 ± 5.2	−7.1 ± 4.4	163
Spring/summer	whole	150	38	7.8 ± 0.6	354.4 ± 9.9	40.3 ± 21	10.7	2072 ± 9	−37 ± 16	−2.7 ± 4.8	81
	north 42°	150	46	7.6 ± 0.5	350.4 ± 8.9	19 ± 15	10.9	2072 ±8	−50 ± 9	−3.1 ± 4.8	98
	south 42°	150	30	7.9 ± 0.5	358.9 ± 9.8	59 ± 14	10.5	2071 ± 7	−28 ± 13	−2.2 ± 4	64

[a]For the calculations we used the time interval Δt, averaged values between cruises for the mixed layer depth (Z), fCO$_2$ in seawater, and changes in temperature and in the fCO$_2$ (ΔfCO$_2$), the Revelle factor for the experimental conditions, the average air-seawater flux following (2) (FCO$_2$), and the average amount of total dissolved inorganic carbon in the mixed layer per area unit (TC_T).

10^{11} m^2 of the POMME area), and this value was lower than values obtained north of 42°N (48% of the total value). The residual daily changes of dissolved inorganic carbon, based on the fCO$_2$, were used here due to the high sampling resolution of the fCO$_2$ when compared to both the lower density and the computed values of C_T.

[30] From the end of March to September (150 days), the increase in the fCO$_2$, up to 59 µatm to the south of 42°N and only 19 µatm to the north (Tables 1 and 2), was outbalanced by the 7.8°C temperature increase (0.87 µatm d^{-1}) and by the input from the air-sea exchange. The high residual term for the POMME area in this period (−2.3 mol m^{-2} or −5.66 Tg C), expressed on a daily basis (−15.5 mmol m^{-2} d^{-1}), was quite similar to the one determined during February and March (−19.1 mmol m^{-2} d^{-1}). However, the drawdown of the C_T north of 42° (40 g C m^{-2}) was twice that south of 42°N, and represents 68% of the total drawdown.

[31] In order to improve our knowledge of the processes accounting for these results, the residual changes over the mixed layer corresponding to the effects of vertical and horizontal transport, $U + H$, and biological activity [Bakker et al., 1997] were considered between the winter and spring cruises. The long period elapsing between the spring and summer cruises, the changing fluxes, entrainments and physical conditions over the whole domain makes computation of the different input inappropriate in this case.

[32] The time averaged 2D field of horizontal advection current was computed considering the mean mixed layer zonal and meridional component of the current [Giordani et al., 2005; G. Caniaux, personal communication, 2004]. Vertical velocity in m/day at the mixed layer base, which

includes the Ekman pumping, was also considered. However, the vertical velocity contribution on the average domain scale can be discounted over the 49 day time elapse between the winter and spring cruises. This particular contribution produces an average deepening of only 1 m, whereas the total decrease in the mixed layer depth in between cruises was over 80 m (Table 1). On the other hand, vertical transport at the mixed layer base produced a local displacement of the water column which reached maximum displacements of 65 m. This is closely related to the field of eddies and located around the transition zone at 41°N. The horizontal transport displaced water within the POMME area, outward and also brought water from the surrounding regions. Owing to the lack of inorganic carbon data outside the POMME area, only the seawater remaining in the area over the 49 days between the two cruises was used in the estimation. Considering the 0.5° × 0.5° resolution in the field of horizontal advection currents, the position of an initial water mass in the winter cruise was determined after the 49 day period. The difference in the concentration of the dissolved inorganic carbon for this water mass between the two positions during winter was used to calculate the rate of change of C_T due to horizontal advection (Table 3). Only 30 points (12 of them north of 42°N) from the initial 120 points in the grid were inside the POMME area after this period and were plotted to estimate the average horizontal advection term (data not shown). The reduced number of data may increase the margin of error in the transport estimate. However, when an average value of C_T was assumed for points located outside of the area, north of 42°N (2094 µmol kg^{-1} (Table 2)) and south of 42°N (2084 µmol kg^{-1} (Table 2)), only 10% variability was to be

Table 3. Observed Daily Changes of fCO$_2$ ($\Delta f/\Delta t$) From Table 2 Related to the Expected Changes of the Surface Warming ($\delta f/\delta T$) (fCO$_2$ at Each Cruise From Table 1 Was Considered in this Case) Together With the Air-Sea Exchange ($\delta f/\delta F$)[a]

	Section	$\Delta f/\Delta t$, µatm d^{-1}	$(\delta f/\delta t)_T$, µatm d^{-1}	$(\delta f/\delta t)_F$, µatm d^{-1}	$(\delta f/\delta t)_R$, µatm d^{-1}	$R_{f\text{CO}2}$, mmol m^{-2} d^{-1}	$U+H$, mmol m^{-2} d^{-1}	NCP, mmol m^{-2} d^{-1} Model	NCP, mmol m^{-2} d^{-1} Experimental
Spring/winter	full	−0.18	0.059	0.144	−0.38	−19.1	−7.6	27	43 ± 20
	north 42°	−0.14	0.072	0.108	−0.32	−18.2	−10.9	29	60.4
	south 42°	−0.21	0.050	0.192	−0.45	−19.2	−3.3	22	38.4
Summer/spring	full	0.27	0.87	0.159	−0.76	−15.5			
	north 42°	0.13	0.87	0.152	−0.89	−22.1			
	south 42°	0.39	0.87	0.165	−0.64	−10.4			

[a]The residual daily change of fCO$_2$ ($\delta f/\delta R$) converted to a net residual daily change of dissolved inorganic carbon ($R_{f\text{CO}2}$) corresponds to the effects of horizontal and vertical advection ($H+U$) and biological activity (expressed as a net community production, NCP) according to (4). Only for the spring and winter cruises each contribution was considered. Values determined during leg 2 winter cruise (March 2001) and $R_C = -\Delta$O$_2$:ΔC = 1.41 [Maixandeau et al., 2005].

observed. The highest C_T gradient determined for the seawater originally north of 42° together with the higher horizontal velocity, accounted for the most significant horizontal advection term in Table 3.

3.5. Biological Processes and fCO$_2$

[33] The biological consumption of the C_T in the upper water explains the negative residual. After considering the inputs of the horizontal and vertical advections to the residual term in (4), the remaining value was given as the result of the variation of carbon as a consequence of the biological activity, and represents the net community production rate (NCP) in the mixed layer of the POMME area. *Maixandeau et al.* [2005; A. Maixandeau et al., Mesoscale and seasonal variability of community production and respiration in the NE Atlantic Ocean, submitted to *Deep-Sea Research, Part I*, 2004] determined the net community production rate integrated over the first 100 m during leg 2. Four stations were sampled during leg 2 of the first cruise, carried out between the winter and spring cruises. The gross community production (GCP) determined by oxygen experiments (24 hours) for the POMME area was 71 ± 16 mmol C m^{-2} d^{-1}, while the dark community respiration (DCR) increased carbon concentration in 31 ± 14 mmol C m^{-2} d^{-1} (after applying an average $R_C = -\Delta O_2:\Delta C = 1.41$ [*Fraga et al.*, 1998]). The NCP for the area during this period was 43.3 ± 20 mmol C m^{-2} d^{-1} (Table 3). This value was close to the value measured at the end of April (leg 2, spring cruise) of 46 mmol C m^{-2} d^{-1}. However, the GCP increased to 112 mmol C m^{-2} d^{-1} [*Maixandeau et al.*, 2005]. *Merlivat et al.* [2001] showed that the bloom started everywhere at the end of March, becoming far less intense by the end of May (except, perhaps, in the extreme north). *Chipman et al.* [1993] reported an NCP value during daytime without time of respiration of 83 ± 17 mmol C m^{-2} d^{-1} during the North Atlantic Bloom Experiment at 47°N in April–May 1989, which is in agreement with the GCP values determined during POMME project. However, as was shown by *Fernández et al.* [2005b], integrated primary production determined by ^{13}C assimilation experiments (12 hour incubation) for stations during the winter and spring cruises (leg 1) showed higher values in front-eddy interaction zones and inside eddies with increased nutrient concentrations than in nonaffected stations. The four sites selected in leg 2 for NCP determinations were located in these areas, and the resulting NCP value of 43 mmol C m^{-2} d^{-1} should be considered a maximum value for the area in March.

[34] The application of the model to profile the carbon dioxide variability in surface waters (4) allowed us to determine a time integrated mean value NCP rates in the mixed layer and to support the calculated contribution of advection to the change in the dissolved inorganic carbon concentrations between cruises. Our model predicts that NCP decreases the inorganic carbon in the mixed layer by about 28 mmol C m^{-2} d^{-1} during the winter and spring cruises, higher north of 42°N than south of 42°N, and in line with the latitudinal variability in primary production [*Fernández et al.*, 2005b]. This value coincides with the maximum determined NCP value of 43 ±

20 mmol m^{-2} d^{-1}. Our model considers the contribution of the advection using modeled mean currents applicable only to water masses moving inside the area and neglects the vertical velocity term. These two factors could also account for the difference observed. However, our model is a true prediction of the various inputs to the observed budget, including an average NCP of 28 mmol C m^{-2} d^{-1}, which makes it the most important contributor to the fCO$_2$ change rate in seawater in the POMME area between February and April 2001.

[35] *Paillet and Mercier* [1997], *Valdivieso da Costa et al.* [2005], *Le Cann et al.* [2005], and *Mémery et al.* [2005] describe the subduction process taking place in the POMME area. They have quantified annual subduction rates S_{ann}, as the annual average volume flux per horizontal area unit across the base of the deepest winter mixed layer, between 50 and 100 m yr^{-1} in the central subtropical gyre, increasing to 100–200 m yr^{-1} when they approached 15° W and 45°N, the POMME area. These values correspond also to the region of formation of subtropical mode water, associated with the southward turn of a part of the North Atlantic Current, with outcrop densities between 26.9 and 27.1. The annual subduction rate for the POMME area north of 42°N where subduction takes place [*Valdivieso da Costa et al.*, 2005; *Mémery et al.*, 2005] accounts for 0.32 Sv (area of 1.0×10^{11} m^2). The inorganic carbon concentration in the mixed layer at the end of winter was $C_{T,w} = 2090 \pm 5$ μmol kg^{-1}, decreasing during the summer cruise down to 2060 ± 10 μmol kg^{-1}. The amount of inorganic carbon subducted in this area at the end of winter ($C_{T,s} = C_{T,w} \times \rho \times S_{ann}$) would account for 0.25 Pg C yr^{-1}. Such an amount of dissolved inorganic carbon represents about 10% of the net global oceanic CO$_2$ sink (2.2 ± 0.7 Pg C yr^{-1}) reported by *Takahashi et al.* [2002] for 1995. This value represents an order of magnitude estimate and shows that this area plays an important role in transporting dissolved CO$_2$ concentration into the inner ocean. Following *Pérez et al.* [2002], the anthropogenic effect in the CO$_2$ content for the surface water was 45 ± 5 μmol kg^{-1} which is similar to that reported by these authors for this region. We calculated that the subducted amount of anthropogenic carbon in the POMME area was 4.6 mol m^{-2} yr^{-1} or 5.4 Tg C yr^{-1}, i.e., about 0.25% of the net global oceanic CO$_2$ sink.

4. Conclusions

[36] Surface fCO$_2$ values determined during late winter, spring and summer over the area covered by the POMME project centered around 42°N, 19°W are strongly modulated by the different effects of temperature, entrainment and biological activity. In spring, the fCO$_2$ values were at their lowest, due to the effect of the biological pump on the deeper and both nutrient and CO$_2$ richer, winter seawater. During the spring and summer, the fCO$_2$ values increased due to the sea surface warming. This increase was smaller than that expected from the temperature contribution, because of the effect of primary production. Between the end of March and September, the fCO$_2$ increased up to 59 μatm to the south of 42°N and only 19 μatm to the north of this latitude. These values were

outbalanced by the 6°–8°C temperature increase and by the air-sea exchange contribution. An important drawdown of C_T was noted, with values higher north of 42° than south of 42°N. North of 42°N, the net community production rates were higher than the values found to the south of 42°N due to the higher nutrient values in the mixed layer.

[37] In the subtropical gyre, the subduction of subpolar mode water plays an important role in transporting inorganic carbon from the surface to deeper layers. Estimated values of subducted inorganic carbon for this area would account for 0.25 Pg C yr^{-1}, i.e., about 10% of the net global oceanic CO$_2$ sink. Moreover, this value indicates an important carbon subduction of anthropogenic origin which is close to 5.4 Tg C yr^{-1}.

References

Assenbaum, M., and G. Reverdin (2005), Near real-time analyses of the mesoscale circulation during the POMME experiment, *Deep Sea Res., Part I*, in press.

Bakker, D. C. E., H. J. W. De Baar, and U. V. Bathmann (1997), Changes of carbon dioxide in surface waters during spring in the Southern Ocean, *Deep Sea Res., Part II*, 44, 91–127.

Bates, N. R. (2001), Interannual variability of oceanic CO$_2$ and biogeochemical properties in the western North Atlantic subtropical gyre, *Deep Sea Res., Part II*, 48, 1507–1528.

Bellerby, R. G. J., D. R. Turner, G. E. Millward, and P. J. Worsfold (1995), Shipboard flow injection determination of sea water pH with spectrophotometric detection, *Anal. Chim. Acta*, 309, 259–270.

Butler, J. H., C. M. Elkins, C. M. Bruson, K. B. Egan, T. M. Thompson, T. J. Conway, and B. D. Hall (1998), Trace gases in and over the West Pacific and East Indian Oceans during the El Niño–Southern Oscillation event of 1987, *Data Rep. ERL-ARL-16*, 104 pp., NOAA Air Resour. Lab., Silver Spring, Md.

Caniaux, G., A. Brut, D. Bourras, H. Giordani, A. Paci, L. Prieur, and G. Reverdin (2005), A 1 year sea surface heat budget in the northeastern Atlantic basin during the POMME experiment: 1. Flux estimates, *J. Geophys. Res.*, 110, C07S02, doi:10.1029/2004JC002596.

Chipman, D. W., J. Marra, and T. Takahashi (1993), Primary production at 47°N and 20°W in the North Atlantic Ocean: A comparison between the ^{14}C incubation method and the mixed layer carbon budget, *Deep Sea Res., Part II*, 40, 151–160.

Clayton, T. D., and R. H. Byrne (1993), Spectrophotometric seawater pH measurements: Total hydrogen ion concentration scale calibration of m-cresol purple and at-sea results, *Deep Sea Res., Part I*, 40, 2115–2119.

Dickson, A. G., and C. Goyet (Eds.) (1994), *Handbook of Methods for the Analysis of the Various Parameters of the Carbon-Dioxide System in Sea Water*, vers. 2, *Rep. ORNL/CDIAC-74*, 180 pp., Dep. of Energy, Washington, D. C.

Dickson, A. G., and F. J. Millero (1987), A comparison of the equilibrium constants for the dissociation of carbonic acid in seawater media, *Deep Sea Res.*, 34, 1733–1743.

Fernández, C. I., P. Raimbault, G. Caniaux, N. Garcia, and P. Rimmelin (2005a), Influence of mesoscale eddies on nitrate distribution during the

POMME program in the north-east Atlantic Ocean, *J. Mar. Syst.*, 55, 155–175.

Fernández, C. I., P. Raimbault, N. Garcia, P. Rimmelin, and G. Caniaux (2005b), An estimation of annual new production and carbon fluxes in the northeast Atlantic Ocean during 2001, *J. Geophys. Res.*, 110, C07S13, doi:10.1029/2004JC002616.

Fraga, F., A. F. Ríos, F. F. Pérez, and F. F. Figueiras (1998), Theoretical limits of oxygen:carbon and oxygen:nitrogen ratios during photosynthesis and mineralisation of organic matter in the sea, *Sci. Mar.*, 62, 161–168.

Giordani, H., G. Caniaux, and L. Prieur (2005), A simplified 3D oceanic model assimilating geostrophic currents: Application to the POMME experiment, *J. Phys. Oceanogr.*, 35, 628–644.

González Dávila, M., J. M. Santana-Casiano, M. J. Rueda, O. Llinás, and E. F. González Dávila (2003), Seasonal and interanual variability of sea-surface carbon dioxide species at the European Station for Time Series in the Ocean at the Canary Islands (ESTOC) between 1996 and 2000, *Global Biogeochem. Cycles*, 17(3), 1076, doi:10.1029/2002GB001993.

Le Cann, B., M. Assenbaum, J.-C. Gascard, and G. Reverdin (2005), Observed mean and mesoscale upper ocean circulation in the mid-latitude northeast Atlantic, *J. Geophys. Res.*, 110, C07S05, doi:10.1029/2004JC002768, in press.

Maixandeau, A., et al. (2005), Microbial community production, respiration, and structure of the microbial food web of an ecosystem in the northeastern Atlantic Ocean, *J. Geophys. Res.*, doi:10.1029/2004JC002694, in press.

Mehrbach, C. C. H. Culberson, J. E. Hawley, and R. M. Pytkowicz (1973), Measurement of the apparent dissociation constants of carbonic acid in seawater at atmospheric pressure, *Limnol. Oceanogr.*, 18, 897–907.

Mémery, L., G. Reverdin, J. Paillet, and A. Oschlies (2005), Introduction to the POMME special section: Thermocline ventilation and biogeochemical tracer distribution in the northeast Atlantic Ocean and impact of mesoscale dynamics, *J. Geophys. Res.*, doi:10.1029/2005JC002976, in press.

Merlivat, L., M. González Dávila, J. M. Santana-Casiano, G. Reverdin, M. Rafizadeh, L. Morvan, A. Beaumont, A. Guillot, and T. Danguy (2001), Mesoscale variability of pCO$_2$ at the sea surface in the northeast Atlantic Ocean as measured by Carioca drifters, in *Proceedings of the 6th International Carbon Dioxide Conference*, pp. 695–698, Sendai, Japan.

Mintrop, L., F. F. Pérez, M. González Dávila, J. M. Santana-Casiano, and A. Körtzinger (2000), Alkalinity determination by potentiometry: Intercalibration using three different methods, *Cien. Mar.*, 26, 23–37.

Paillet, J., and M. Arhan (1996), Shallow pycnoclines and mode water subduction in the eastern North Atlantic, *J. Phys. Oceanogr.*, 26, 96–114.

Paillet, J., and H. Mercier (1997), An inverse model of the eastern North Atlantic general circulation and thermocline ventilation, *Deep Sea Res., Part I*, 44, 1293–1328.

Pérez, F. F., M. Alvarez, and A. F. Ríos (2002), Improvements of the back-calculation technique for estimating anthropogenic CO$_2$, *Deep Sea Res., Part I*, 49, 859–875.

Poisson, A., N. Metzl, C. Brunet, B. Schauer, B. Bres, D. Ruiz-Pino, and F. Louanchi (1993), Variability of sources and sinks of CO$_2$ in the western Indian and Southern Oceans during the year 1991, *J. Geophys. Res.*, 98, 22,759–22,778.

Reverdin, G., M. Assenbaum, and L. Prieur (2005), Eastern North Atlantic Mode Waters during POMME (September 2000–2001), *J. Geophys. Res.*, 110, C07S04, doi:10.1029/2004JC002613.

Ríos, A. F., F. F. Pérez, M. Alvarez, L. Mintrop, M. González-Dávila, J. M. Santana-Casiano, N. Lefevre, and A. J. Watson (2005), Seasonal sea-surface carbon dioxide in the Azores area, *Mar. Chem.*, 96, 35–51.

Takahashi, T., J. Olafsson, J. G. Goddard, D. W. Chipman, and S. C. Sutherland (1993), Seasonal variation of CO$_2$ and nutrients in the high-latitude surface oceans: A comparative study, *Global Biogeochem. Cycles*, 7, 843–878.

Takahashi, T., T. T. Takahashi, and S. C. Sutherland (1995), An assessment of the role of the North Atlantic as a CO$_2$ sink, *Philos. Trans. R. Soc. London, Ser. B*, 348, 143–152.

Takahashi, T., R. A. Feely, R. Weiss, R. H. Wanninkhof, D. W. Chipman, S. C. Sutherland, and T. T. Takahashi (1997), Global air-sea flux of CO$_2$: An estimate based on measurements of sea-air pCO$_2$ differences, *Proc. Natl. Acad. Sci.*, 94, 8292–8299.

Takahashi, T., R. H. Wanninkhof, R. A. Feely, R. F. Weiss, D. W. Chipman, N. Bates, J. Olafsson, C. Sabine, and S. C. Sutherland (1999), Net sea-air CO$_2$ flux over the global oceans: An improved estimate based on the sea-air pCO$_2$ difference, in *Proceedings of the Second International Symposium: CO$_2$ in the Oceans*, edited by

Y. Nojiri, pp. 9–14, Cent. for Global Environ. Res. Natl. Inst. for Environ. Stud., Tsukuba, Japan.

Takahashi, T., et al. (2002), Global sea-air CO$_2$ flux based on climatological surface ocean pCO$_2$ and seasonal biological and temperature effects, *Deep Sea Res., Part II*, *49*, 1601–1622.

Valdivieso da Costa, M., H. Mercier, and M. Tréguier (2005), Effects of the mixed-layer time variability on kinematic subduction rate diagnostics, *J. Phys. Oceangr.*, *35*, 427–443.

van Aken, H. M. (2001), The hydrography of the mid-latitude northeast Atlantic Ocean, part III: The subducted thermocline water mass, *Deep Sea Res., Part I*, *48*, 237–267.

Wanninkhof, R. (1992), Relationship between wind speed and gas exchange over the ocean, *J. Geophys. Res.*, *97*, 7373–7382.

Wanninkhof, R., and K. Thoning (1993), Measurement of fugacity of CO$_2$ in surface water using continuous and discrete sampling methods, *Mar. Chem.*, *44*, 189–204.

––––––––––––––––––

L. Barbero-Muñoz, E. V. Dafner, M. González Dávila, and J. M. Santana-Casiano, Facultad de Ciencias del Mar, Universidad de Las Palmas de Gran Canaria, E-35017 Las Palmas, Spain. (leticia.barbero101@doctorandos. ulpgc.es; evgeny@hawaii.edu; mgonzalez@dqui.ulpgc.es; jmsantana@ dqui.ulpgc.es)

L. Merlivat, Laboratoire d'Océanographie Dynamique et de Climatologie/Centre National de la Recherche Scientifique, Université Paris VI, 4, place Jussieu, F-75252 Paris Cedex 06, France. (merlivat@lodyc.jussieu.fr)